ORIGINAL PAPER

Multiwalled carbon nanotubes coated with cobalt(II) sulfide nanoparticles for electrochemical sensing of glucose via direct electron transfer to glucose oxidase

Juan Li[1] · Yiting Liu[1] · Xiao Tang[1] · Lijia Xu[1] · Lingfeng Min[2] · Yadong Xue[3] · Xiaoya Hu[1] · Zhanjun Yang[1]

Abstract

Multiwalled carbon nanotubes coated with cobalt(II) sulfide nanoparticles were prepared and used for immobilization of glucose oxidase (GOx) to obtain an electrochemical glucose biosensor. The nanocomposite was synthesized through an in-situ hydrothermal method and characterized by X-ray diffraction, scanning electron microscopy, transmission electron microscopy, and electrochemical impedance spectroscopy. The results show that the nanocomposite possesses a large specific surface area and apparently enhances the direct electron transfer between GOx and the surface of the electrode, best at a potential near -0.43 V (vs. SCE). The immobilized GOx retains its good bioactivity even at a high surface coverage of 30 pmol cm^{-2}. Under the optimum conditions. The biosensor exhibits a wide linear range (from 8 μM to 1.5 mM), a high sensitivity (15 mA M^{-1} cm^{-2}), and a 5 μM detection limit (at S/N = 3). The sensor is selective, acceptably repeatable, specific and stable.

Keywords Metal sulfide nanoparticles · Carbon nanotubes · Enzyme · Modified electrode · Direct electrochemistry

Introduction

The rapid and accurate glucose detection is of great significance to diagnose and treat diabetes [1, 2]. There are many methods for determination of glucose concentration, such as high-performance liquid chromatography, spectrophotometry, optical rotation, colorimetry, etc. Electrochemical biosensors

✉ Lingfeng Min
  minlingfeng@126.com

✉ Yadong Xue
  xueyadong@zju.edu.cn

✉ Zhanjun Yang
  zjyang@yzu.edu.cn

1   School of Chemistry and Chemical Engineering,, Yangzhou University, Yangzhou 225002, People's Republic of China

2   Department of Laboratory Medicine and Clinical Medical College of Yangzhou University, Subei Peoples' Hospital of Jiangsu Province, Yangzhou 225001, People's Republic of China

3   Jinhua Hospital, Zhejiang University School of Medicine, Hangzhou, China

have been widely applied in many fields due to their high sensitivity, fast analysis speed, high selectivity, simple instrument operation as well as low cost [3, 4]. More and more attention has been paid on the development of the third generation glucose biosensor through direct-electron-transfer (DET) of cofactor flavin-adenine dinucleotide (FAD) of glucose oxidase (GOx) on the electrode surface [5]. However, the DET of oxidation of FADH$_2$ or reduction of FAD of enzymes at conventional electrodes is hard to realize [6]. This is because that the redox centers of GOx are deeply seated in the cavity of enzyme molecules and not easily accessible for the conduction of electrons from the electrode surface [7]. It has been found that that nanostructured material-modified electrode can accelerate the DET due to its electron mediated function [8, 9]. In the past decades, carbon [10, 11], metal [12, 13] and semiconductor nanomaterials [14, 15] have been explored to promote the DET of GOx on the surface of the electrode.

Carbon nanotubes (CNTs) have attracted interest in electrochemical biosensor fields. This is due to their excellent electrical conductivity, unique mechanical properties, high specific surface area, fast electron transport, chemical stability and strong adsorption ability [16]. Many studies have shown that carbon nanotubes are quite useful for the

immobilization of GOx and electron transferring process [17, 18], which can promote the direct electrochemistry of biomolecules [19]. However, owing to the presence of a relatively inert surface, it is almost inevitable that CNTs need to be modified before they are used as carriers for electrochemical biosensing [20]. According to previous researches, CNTs-based hybrid composites have become more and more attractive because the functionalized materials may generate synergy effect and enhance their performance in sensing application [21, 22]. However, the poor solubility in most common solvents of CNTs-based materials and their tendency to form aggregates hindered the applications in fabrication of biosensor device [23]. Therefore, the development of novel and efficient CNTs-based composite for DET-based electrochemical biosensors is still a challenge.

Cobalt sulfide, as an important semiconductor nanomaterial, has been applied in various fields due to its unique magnetic, catalytic, and electrical properties as well as its unique stoichiometric ratio (CoS, CoS_x, CoS_2, Co_3S_4, Co_9S_8, etc.) [24, 25]. A new type of nanocomposite was synthesized by assembling cobalt sulfide nanoparticles onto multi-walled carbon nanotubes (CoS-MWCNTs) through in situ hydrothermal method. To the best of our knowledge, the preparation of electrochemical glucose biosensor using CoS-MWCNTS nanocomposite to immobilize GOx has not been reported so far. The nanocomposite has a large specific surface area, high surface free energy, good biocompatibility, excellent ability of immobilizing protein molecules. These properties further make the modified electrode have a special catalytic ability to promote DET of the GOx on the surface of electrode. As a result, the constructed electrochemical glucose biosensor shows high sensitivity and low detection limit for glucose, and can be successfully applied in the quantitative detection of glucose at the potential of −0.43 V. The CoS-MWCNTS nanocomposite provides a new alternative for the preparation of electrochemical biosensors.

Materials and methods

Materials and reagents

Glucose oxidase (from *Aspergillus niger*, ≥100 U mg^{-1}), D-(+)-Glucose, and Nafion were supplied by Sigma-Aldrich (http://www.sigma-aldrich.com). Multi-walled carbon nanotubes (MWCNTs, diameter: 10–20 nm, length: 5–15 μm) were purchased from Shenzhen Nanotech Port Co., Ltd. (China, http://www.nanotubes.com.cn). Cobalt(II) chloride hexahydrate ($CoCl_2·6H_2O$, AR), thiocarbamide (CH_4N_2S, AR), and ethylene glycol (($CH_2OH)_2$, AR) were bought from Sinopharm Chemical Reagent Co., Ltd. (China, https://www.sinoreagent.com). The electrolyte is phosphate buffer which being obtained by mixing 0.1 M Na_2HPO_4 with 0.

1 M NaH_2PO_4 solution. All other chemicals and reagents are of analytical grade and commercially available. Distilled water was used for all experiments.

Apparatus

Electrochemical measurements were carried out on a CHI 852C electrochemical workstation (Shanghai Chenhua Co. Ltd., China). All measurements were carried out using a three-electrode system. This system includes a modified glassy carbon electrode (GCE) as working electrode, a saturated calomel electrode (SCE) as reference electrode, and a platinum sheet as auxiliary electrode. Cyclic voltammetry and amperometric measurements were carried out in 10.0 mL of phosphate buffer. All pH values were measured using an S-25 digital pH-meter with glass combination electrode. Electrochemical impedance spectroscopy (EIS) analysis was performed on an Autolab PGSTAT30 (The Netherlands) using a solution of 0.10 M KCl containing 5.0 mM $K_3[Fe(CN)_6]/K_4[Fe(CN)_6]$. The amplitude of the applied sine wave potential is 5 mV and the frequency range was from 0.05 to 10 kHz at a bias potential of 190 mV. Field-emission scanning electron microscope (FESEM) used to characterize the surface morphology of samples and modified electrodes were obtained with a Zeiss Supra 55 scanning electron microscope (Germany) at an acceleration voltage of 5 kV. Transmission electron microscopy (TEM) was conducted on a FEI Tecnai G2 F30 S-TWIN field-emission transmission electron microscopy (USA) at an acceleration voltage of 300 kV. X-ray diffraction (XRD) pattern was recorded on D8 Advance X-ray diffractometer (Bruker Co., Germany) at room temperature. Raman spectra were carried out on Renishaw Invia Raman spectroscope.

Preparation of CoS-MWCNT nanocomposite

Firstly, 1.0 mmol $CoCl_2·6H_2O$ (0.2379 g) and 4.0 mmol $CS(NH_2)_2$ (0.3045 g) were dissolved in a mixed solvent including 20 mL of distilled water and 5 mL of ethylene glycol under vigorous stirring for 30 min. 15 mg of MWCNTs were then dissolved into the above solution. After ultrasonic dispersion for 1 h, the black suspension was transferred into a 60 mL Teflon-lined stainless-steel autoclave. The autoclave was tightly sealed and maintained at 180 °C for 15 h. Then, the product was centrifuged and washed three times with distilled water and absolute ethanol after being naturally cooled down to environmental temperature. Finally, CoS-MWCNTs nanocomposite was obtained under vacuum drying 12 h at 60 °C. For comparison, the CoS samples were also prepared via a similar synthesis process without adding MWCNTs.

Preparation of the electrochemical enzymatic biosensor

The GCE was firstly polished with 0.3 and 0.05 μm alumina slurry (Buhler) in turn, and rinsed thoroughly with distilled water to remove residual alumina slurry. Then, it was sonicated in 1:1 nitric acid-water (*v/v*) solution, acetone and distilled water and finally dried with high purity nitrogen stream before modification to prepare a pretreated GCE. Next, 1.0 mg of CoS-MWCNTs was dispersed in 1.0 mL distilled water with ultrasonication, and then 10.0 mg of GOx powder was added into the CoS-MWCNTs suspension and stirred gently for 15 min. The resultant suspension was subsequently dropped on the pretreated GCE surface and dried at 4 °C in a refrigerator. Afterwards, 5.0 μL of 0.5% Nafion solution was dropped on the surface of GOx/CoS-MWCNTs/GCE to finally obtain the GOx/CoS-MWCNTs /Nafion electrode. When not in use, the enzyme biosensor was stored in pH 7.0 PBS at 4 °C in refrigerator.

Results and discussion

Characterizations of the CoS-MWCNTs and glucose biosensor

Field-emission scanning electron microscopy was used to investigate the surface morphology of the CoS samples and CoS-MWCNTs composite (shown in Fig. 1). It can be clearly seen from Fig. 1a that CoS shows a flower-like microsphere with a diameter of 3 to 5 μm, which is made up of numerous cross-linked nanoflakes with a smooth surface and a thickness of about 20 nm. Compared with pure CoS microspheres, the SEM image of CoS-MWCNTs composite (Fig. 1b) shows that CoS nanoparticles uniformly grows on the wall of the MWCNTs. The particle size of the CoS nanoparticles is much smaller than that of pure CoS samples with a diameter of about 150 nm. Such a significant change should be ascribed to the presence of oxygenous groups (such as C-O, C=O and O-C=O) on the MWCNTs, which allows Co^{2+} to be selectively and uniformly distributed on MWCNTs. In addition, the carbon nanotube as a carrier can inhibit the growth of the CoS nucleus, thereby controlling the size of the CoS particles in the nano level. TEM image of CoS-MWCNTs composite (shown in Fig. 1c) also clearly reveals the structure of nanotubes supported CoS nanoparticles with a solid inner structure. In addition, the elemental distribution of the CoS-MWCNTs is further investigated by EDX mappings. Figure 1d–g show the homogeneous distribution of C, Co and S in the material, confirming that CoS nanoparticles have good contact with MWCNTs.

The crystal structure of CoS and CoS-MWCNTs samples are investigated by powder X-ray diffraction (XRD). As shown in Fig. 2a, the four diffraction peaks of CoS and CoS-MWCNTs are located at 30.6, 35.3, 46.9 and 54.4°. This can be indexed to the (100), (101), (102) and (110) planes of the hexagonal crystal phase (JCPDS card No. 65–8977, space group: *P63/mmc*), respectively. A diffraction peak of CoS-MWCNTs at about 2θ of 26.0° is corresponded to the (002) crystal plane of graphitized carbon. This indicates the presence of several stacked multi-walled carbon nanotubes

Fig. 1 SEM images of pure CoS microspheres (**a**), CoS-MWCNTs nanocomposite (**b**); TEM image of CoS-MWCNTs nanocomposite (**c**); Annular dark-field STEM image and the corresponding EDX elemental mappings of C, Co, and S in CoS-MWCNTs nanocomposite (**d-g**)
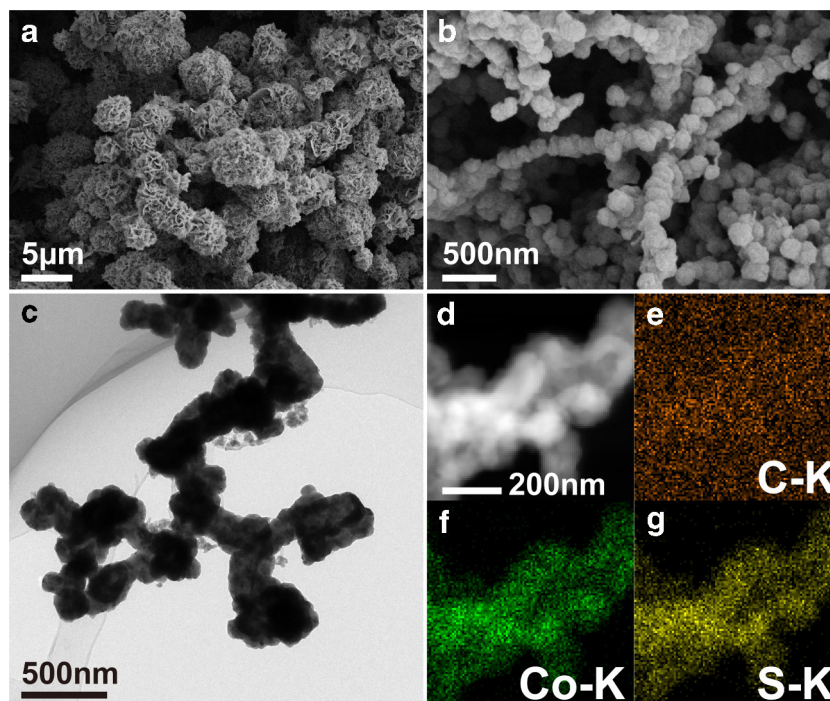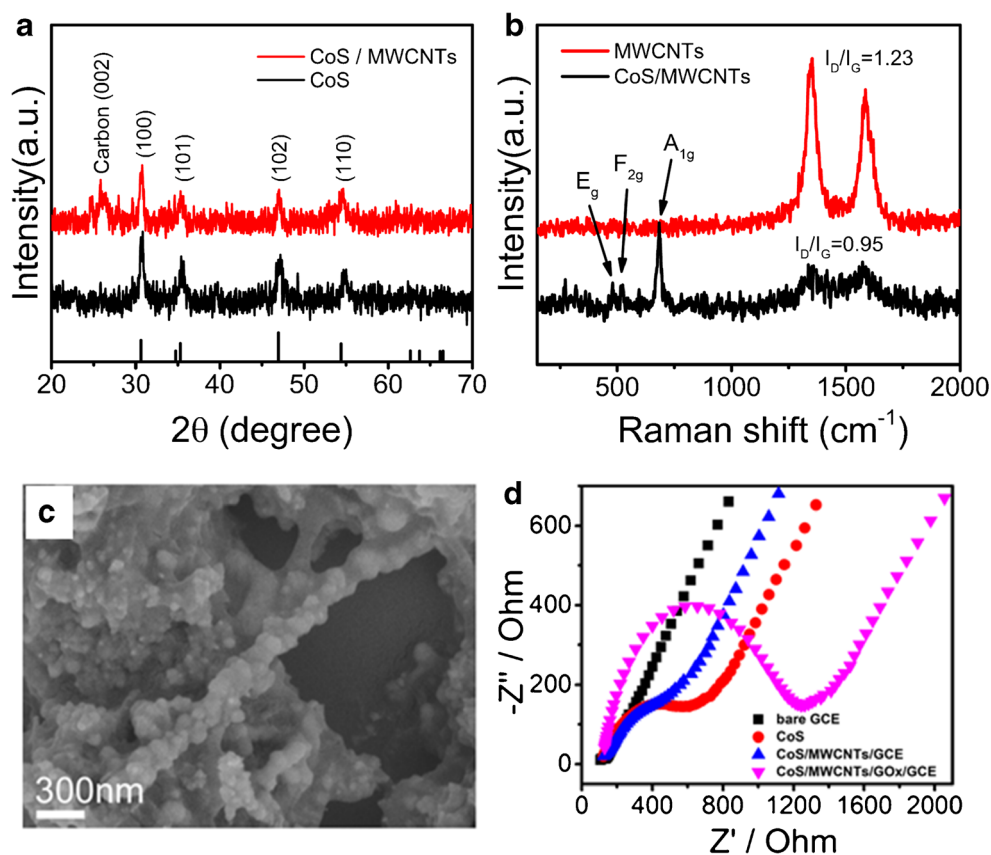
Fig. 2 **a** XRD pattern and (**b**) Raman spectra of pure CoS microspheres and CoS-MWCNTs nanocomposite, **c** SEM image of GOx/CoS-MWCNTs and (**d**) Nyquist plots of EIS for bare, CoS, CoS-MWCNTs and GOx/CoS-MWCNTs modified GCEs

within the CoS-MWCNTs material. Raman spectroscopy was used to analyze the microstructure of MWCNTs and CoS-MWCNTs (Fig. 2b). For MWCNTs, we can observe that there are two characteristic peaks at 1351 and 1586 cm^{-1}, which are assigned to disordered (D) carbon and graphite (G) carbon structure, respectively. The intensity ratio of I_D/I_G for CoS-MWCNTs nanocomposite was calculated to be 1.09, slightly lower than that of MWCNTs 1.23, suggesting that the CoS-MWCNTs nanocomposite increases the graphitic crystallinity in the carbon component due to the introduction of CoS. Compared with the spectrum of MWCNTs, three other characteristic peaks of CoS-MWCNTs at 479, 521 and 682 cm^{-1} can be ascribed to the typical E_g, F_{2g}, and A_{1g} vibration modes of CoS [26], further confirming the presence of hexagonal CoS nanoparticles and MWCNTs.

CoS-MWCNTs nanocomposite was successfully synthesized using in situ hydrothermal reaction and subsequently employed to immobilize GOx to prepare electrochemical enzyme biosensor. Compared with the SEM image of CoS-MWCNTs nanocomposite (Fig. 1b), the SEM image of GOx-loaded CoS-MWCNTs shows a different surface morphology after the immobilization of GOx molecules (Fig. 2c). It can be clearly seen that enzyme molecules were uniformly aggregated on the surface of CoS-MWCNTs, indicating the successful immobilization of GOx.

The electrochemical impedance spectroscopy (EIS) was used to characterize the interface properties of different modified electrode. As shown in Fig. 2d, all of their Nyquist plots are constituted with a semicircular arc at high frequency region and an inclined line at low frequency region, which correspond to the electron-transfer limited process and diffusional-limited process, respectively. The semicircle at high frequency affects the electron transfer kinetics of the electrode/electrolyte interface, and its diameter corresponds to the charge transfer resistance (R_{ct}). It can be clearly observed that the CoS/GCE shows a larger R_{ct} than that of bare GCE, demonstrating that the CoS film has formed on the surface of GCE. It is worth noting that CoS-MWCNTs/GCE exhibits relative lower R_{ct} value than that of CoS/GCE. This indicates that the presence of MWCNTs improves the electrical conductivity and promotes the electron transport kinetics of the CoS-MWCNTs. The R_{ct} value of GOx/CoS-MWCNTs/GCE shows a significant increased R_{ct} value after the modification of GOx molecular. The reason for the obvious change is that the protein layer formed on the surface of the electrode hinders the diffusion of ferricyanide probe toward the electrode surface. This also indicates that the GOx is successfully immobilized on the CoS-MWCNTs film.

The electrochemical behavior of the glassy carbon electrode (GCE) modified with GOx/CoS-MWCNT

To examine possibility of DET of GOx onto CoS-MWCNTs/GCE, cyclic voltammograms (CVs) of different modified GCEs in 0.1 M N$_2$-saturated pH 6.0 phosphate buffer (scan rate: 100 mV s^{-1}) are examined in Fig. 3. The CV curves of Nafion/GCE and Nafion/CoS-MWCNTs/GCE show no obvious peaks, which suggests that there is no electrochemical redox process without enzymes. However, the Nafion/CoS-MWCNTs/GCE shows higher background current compared with Nafion/GCE, which may be attributed to the larger surface area of CoS-MWCNTs nanocomposite [16]. Although the CV curve of Nafion/GOx/GCE shows a pair of redox peak, the current response is relatively weak. This is because that it is difficult to transfer electrons to the electrode surface due to deeply location of FAD of GOx molecule in the cavity of enzymes. Compared with Nafion/GOx/GCE and Nafion/GOx-CoS/GCE, GOx/CoS-MWCNTs modified electrode has a pair of significant and well-defined redox peaks at −0.443 V and −0.396 V. This result suggests that CoS-MWCNTs can reduce electrical contact between redox-active centers of enzyme and the electrode surface, and thus enhance the direct electron transfer process [27]. The reduction peak current of Nafion/GOx-CoS-MWCNTs /GCE is 2.2 times larger than that of Nafion/GOx/GCE, which may be due to the larger specific surface area and good conductivity [1].

Fig. S1A shows the electrochemical behavior of Nafion/GOx-CoS-MWCNTs/GCE at different scan rates range from 10 to 300 mV s^{-1}. As seen from the inset of Fig. S1A, both of anodic peak current (I_{pa}) and cathodic peak current (I_{pc}) increase with the increase of scan rate, and the potential of redox peaks keep no obvious shift. The anodic and cathodic peak currents displays a linear response to the scan rate, and the
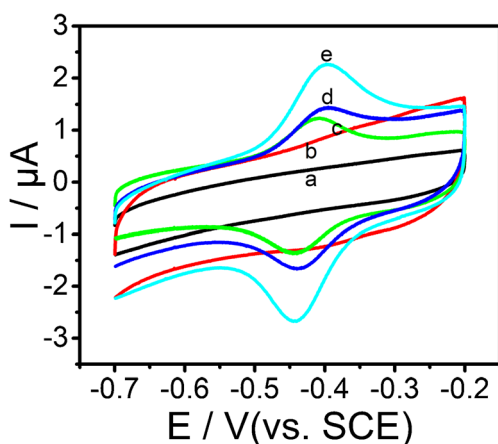
linear regression equations are $I_{pa} = 0.2996 + 0.0070v$, R^2 = 0.9411 and $I_{pc} = -0.2273 - 0.0087v$, R^2 = 0.9696. The ratio of I_{pa}/I_{pc} is close to 1, which indicates that the direct electrochemistry of GOx at CoS-MWCNTs/GCE is a quasi-reversible surface-controlled process [28, 29]. What's more, the surface coverage (Γ^*) of the GOx molecules on the surface of the Nafion/CoS-MWCNTs modified electrode can be obtained according to the equation $\Gamma^* = Q/nFA$ (where Q is the charge consumed in the reaction, n is the number of electrons transferred, F is the Farady constant, and A is the electrode area). The Γ^* of GOx molecules on the surface of Nafion/CoS-MWCNTs modified electrode was calculated to be 2.97 × 10^{-11} mol cm^{-2} from its integration of reduction peak at 100 mV s^{-1}. The value is larger than those of 1.60 × 10^{-11} mol cm^{-2} at GOx/SnS$_2$/Nafion/GCE [15] and 9.8 × 10^{-12} mol cm^{-2} at GOx/Au nanoparticles/carbon paste electrode [12]. The logarithm of cathodic peak current versus the logarithm of scan rate exhibits a linear relationship (inset b of Fig. S1A). The linear regression equation is $\log I_{pc} = -1.5725 + 0.8182\log v$, R^2 = 0.9894), and the slope is close to the theoretical slope of the thin-layer electrochemical behavior.

Cyclic voltammetric responses of Nafion/GOx-CoS-MWCNTs/GCE is closely related to the pH of the solution. Fig. S1B shows CVs of Nafion/GOx-CoS-MWCNTs/GCE within pH range of 4.0 to 9.0, and both the anodic peak and cathodic peak potentials shifted negatively with the increase of solution pH. The formal potential has a linear relationship with the solution pH (inset a of Fig. S1B), and the slope of −48.1 mV/pH is close to the theoretical value of −58.6 mV pH^{-1} reported previously [30]. This suggests that same-proton coupled same-electron transfer participates in the process of redox reaction according to Eq. 1. In addition, the current response of redox peaks reaches the maximum at pH 6.0 (inset b of Fig. S1B), demonstrating the optimal solution pH value for DET of immobilized GOx. To a certain degree, the decreased proton concentration at higher pH value results in a decrease in current response, while the decrease in current response maybe result from lower biological activity of the immobilized enzyme at lower pH value.

$$GOx(FAD) + 2e^- + 2H^+ \leftrightarrow GOx(FADH_2) \qquad (1)$$
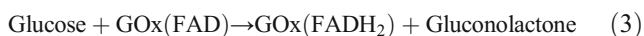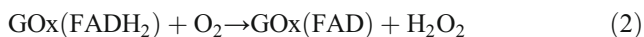
The mechanism of the determination of glucose

The mechanism of DET-based glucose detection is studied by examining CVs of Nafion/CoS-MWCNTs/GCE and Nafion/GOx-CoS-MWCNTs/GCE in nitrogen-saturated and air-saturated pH 6.0 phosphate buffer with or without glucose. As shown in Fig. 4a, whether in nitrogen- or air-saturated PBS, no obvious peaks are observed at Nafion/CoS-MWCNTs/GCE, and the peak current is almost unchanged

Fig. 3 Cyclic voltammograms for (**a-e**) bare GCE, Nafion/CoS-MWCNTs/GCE, Nafion/GOx/GCE, Nafion/GOx/CoS/GCE and Nafion/GOx/CoS-MWCNTs/GCE in N$_2$-saturated 0.1 M pH 6.0 PBS at a scan rate of 100 mV s^{-1}

Fig. 4 Cyclic voltammograms of (**a**) Nafion/CoS-MWCNTs/GCE and (**b**) Nafion/GOx-CoS-MWCNTs/GCE in 0.1 M pH 6.0 N$_2$-saturated PBS and air-saturated PBS including 0, 0.5 and 1.0 mM glucose at a scan rate of 100 mV s^{-1}
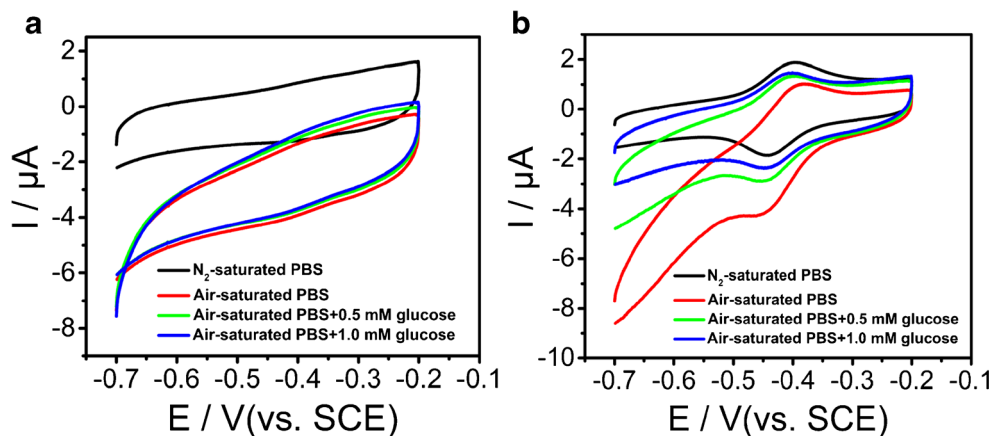
with the addition of glucose. In contrast with the situation mentioned above, a pair of clear and well-defined redox peaks at Nafion/GOx-CoS-MWCNTs/ GCE are observed in both nitrogen-saturated solution and air-saturated solution (shown in Fig. 4b). Nevertheless, it can be observed that the reduction peak current is larger in air-saturated PBS compared with the corresponding peak in N$_2$-saturated PBS. This demonstrates that GOx (FADH$_2$) produced by electrochemical reaction can electrocatalyze the reduction of dissolved oxygen to form GOx (FAD) and hydrogen peroxide [12]. With the decrease of dissolved oxygen, hydrogen peroxide would increase gradually in the process of electrocatalysis. The above phenomenon can be interpreted according to Eqs. (1) and (2).

$$GOx(FADH_2) + O_2 \rightarrow GOx(FAD) + H_2O_2 \qquad (2)$$

$$Glucose + GOx(FAD) \rightarrow GOx(FADH_2) + Gluconolactone \qquad (3)$$

In the presence of dissolved oxygen, the reduction peak current of Nafion/GOx-CoS-MWCNTs/GCE decreases

gradually with the increase of glucose concentration, which is caused by electrocatalytic reaction. Such electrocatalytic reaction inhibits the enzyme-catalyzed reaction between GOx (FAD) and glucose according to following Eq. (3). Therefore, the continuous addition of glucose leads to a decrease in the concentration of GOx (FAD), thereby causing the gradually decrease of reduction current. The results above suggest that the Nafion/GOx-CoS-MWCNTs/GCE can be used as a biosensor to sense glucose.

Performance of the biosensor

Figure 5a shows the amperometric response curve at Nafion/GOx-CoS-MWCNTs/GCE on the successive addition of different concentrations of glucose solution to 10 mL of pH 6.0 air-saturated PBS at an optimal voltage of −0.43 V. The enzyme biosensor reaches 96% of steady-state current just within the time of 5 s. Obviously, the peak current responses increase with the increase of
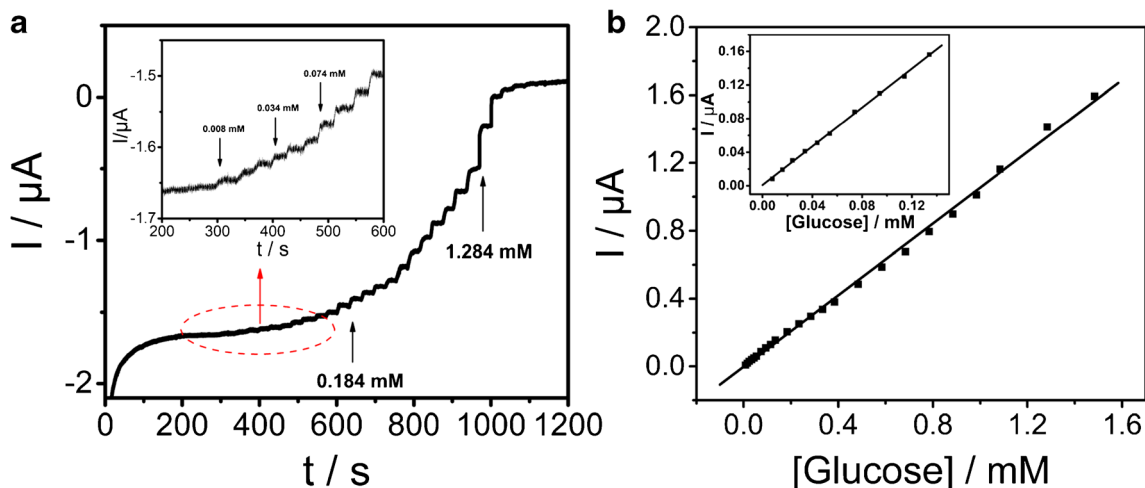
Fig. 5 **a** Typical steady-state response of the Nafion/GOx-CoS-MWCNTs/GCE on successive addition of glucose into air-saturated 0.1 M pH 6.0 PBS at the applied potential of −0.43 V, and (**b**) calibration plot of Nafion/GOx-CoS-MWCNTs/GCE for glucose

glucose content. The calibration plot (Fig. 5b) of the biosensor displays a linear range from 0.008 to 1.5 mM for glucose accompanied by a correlation coefficient of 0.9975 and a high sensitivity of 14.96 ± 0.5 mA·M^{-1}·cm^{-2}. The detection limit is calculated to be 5 μM at a signal-to-noise of 3. The present glucose biosensor is compared with other glucose biosensors reported in recent literatures, including the detection potential, the sensitivity, the detection limit and linear range, which are listed in Table 1. By contrast, it is found that the biosensor based on Nafion/GOx-CoS-MWCNTs/GCE shows satisfactory performance parameters, which is superior to many other biosensors reported previously. The excellent assay performance of the glucose biosensor is ascribed to the large specific surface area and good conductivity of the CoS-MWCNTs composite.

Reproducibility and stability

The precision of the biosensor was investigated in detail by the current response of the same modified electrode in PBS solution containing 0.1 mM glucose. Under the same conditions, five repetitive measurements were conducted with the Nafion/GOx-CoS-MWCNTs/GCE with a relative standard deviation of 2.0%. Then, under the optimized conditions, five enzyme electrodes produced repeatedly were investigated by measuring 0.1 mM glucose, and the relative standard deviation is 6.5%, suggesting good fabrication reproducibility. The Nafion/GOx-CoS-MWCNTs/GCE can be stored in an environment of 4 °C when not in use. The current response of the enzyme electrodes reduced by 7.0% after 30 days, indicating the acceptable storage stability of the Nafion/GOx-CoS-MWCNTs/GCE.
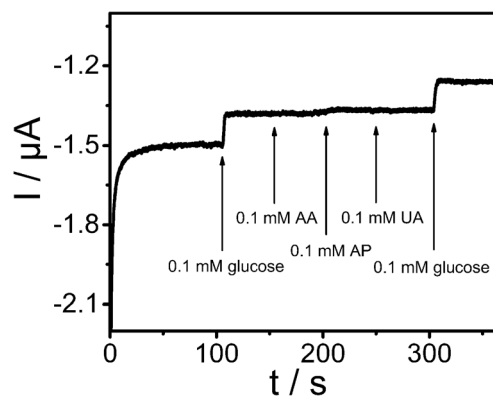

Fig. 6 Amperometric response of the Nafion/GOx-CoS-MWCNTs/GCE to 0.1 mM glucose, 0.1 mM AA, 0.1 mM AP and 0.1 mM UA in pH 6.0 PBS solution at the applied potential of −0.43 V

Interference study and determination of glucose in human serum samples

Several common electroactive interferants such as ascorbic acid (AA), p-acetamidophenol (AP), uric acid (UA) were chosen to examine the selectivity of the Nafion/GOx-CoS-MWCNTs/GCE at −0.43 V applied potential. As shown in Fig. 6, an obvious current response was observed when 0.1 mM glucose was added to phosphate buffer (pH 6.0). However, there is no significant change in peak current upon the continuous addition of 0.1 mM AA, 0.1 mM AP and 0.1 mM UA. Then, 0.1 mM glucose was injected again into the above solution, the current appears again and the response value is very similar to the value obtained in the absence of an interfering substance. The results above demonstrate that the glucose biosensor based on CoS-MWCNTs nanocomposite possesses high selectivity toward glucose.

To evaluate the practical application of the glucose biosensor, the glucose level in human serum samples was analyzed

Table 1 Comparison of analytical performance between Nafion/GOx-CoS-MWCNTs/GCE and other modified electrodes

Electrode	Applied potential (V)	Sensitivity (mA M^{-1} cm^{-2})	Detection limit (mM)	Linear range (mM)	Reference
GOx/CoS-MWCNTs/Nafion/GCE	−0.43	14.96	0.005	0.008–1.5	This work
GOx/CNTs-chitosan/GCE	+0.40	7.36	–	0–7.8	[31]
GOx/SnS$_2$/Nafion/GCE	−0.45	7.6	0.01	0.025–1.1	[15]
GOx/Pt-CNT/GCE	−0.1	–	0.055	0.16–11.5	[32]
GOx/G-CdS/GCE	−0.335	1.76	0.7	2.0–16	[33]
GOx/CNT–AuNPs–ZnS HSs/GCE	+0.50	–	0.01	0.02–7.0	[34]
GOx-Ag-ZnO HNPs/GCE	–	18.7	0.005	0.01–1.5	[35]

CNTs: carbon nanotubes

G: graphene

AuNPs: Au nanoparticles

HSs: hollow spheres

HNPs: Hybrid nanorods

by the present enzyme electrode. Human serum samples were received from Yangzhou Friendship Hospital without any sample pretreatment except a dilution step. When the glucose concentration in human serum samples was more than 1.5 mM, the serum samples were diluted properly using phosphate buffer (pH 7.0). Subsequently, the results tested by the present method are compared with the values from the hospital. The test results for human serum samples are shown in Table S1, and the relative errors between two methods are no more than 7.4%, suggesting that the biosensor can measure glucose accurately in the tested real samples.

Conclusion

An electrochemical glucose biosensor was developed by immobilizing GOx on CoS-MWCNTs nanocomposite modified glassy carbon electrode. CoS-MWCNTs nanocomposite provides a large specific surface area and a favorable biological microenvironment for the direct electrochemistry of GOx. A pair of redox peaks is obtained from the cyclic voltammogram of Nafion/GOx-CoS-MWCNTs/ GCE, corresponding to a quasi-reversible surface-controlled process with the same-proton and the same-electron transfer. CoS-MWCNTs nanocomposite not only retains the bioactivity of the immobilized enzyme but also promotes the DET between GOx and the electrode surface. The immobilized GOx retains high affinity and sensitivity to glucose. The enzyme biosensor exhibits wide linear range, high sensitivity, low detection limit, good reproducibility and stability for the detection of glucose. The biosensor can be applied to the determination of glucose in human serum samples. This work provides an effective material for immobilization of proteins and the development of biosensors.

References

1. Dai H, Zhong YH, Wu XY, Hu RX, Wang L, Zhang YC, Fan GK, Hu XY, Li J, Yang ZJ (2018) Synthesis of perovskite-type SrTiO$_3$ nanoparticles for sensitive electrochemical biosensing applications. J Electroanal Chem 810:95–99

2. Steiner MS, DuerkopA WOS (2011) Optical methods for sensing glucose. Chem Soc Rev 40:4805–4839

3. Wang J (2006) Electrochemical biosensors: towards point-of-care cancer diagnostics. Biosens Bioelectron 21:1887–1892

4. Hahn YB, Ahmad R, Tripathy N (2012) Chemical and biological sensors based on metal oxide nanostructures. Chem Commun 48: 10369–10385

5. Karyakin AA (2012) Principles of direct (mediator free) bioelectrocatalysis. Bioelectrochemistry 88:70–75

6. Shan CS, Yang HF, Song JF, Han DX, Ivaska A, Niu L (2009) Direct electrochemistry of glucose oxidase and biosensing for glucose based on graphene. Anal Chem 81:2378–2382

7. Wang ZY, Liu SN, Wu P, Cai CX (2009) Detection of glucose based on direct electron transfer reaction of glucose oxidase immobilized on highly ordered polyaniline nanotubes. Anal Chem 81:1638–1645

8. You H, Mu ZD, Zhao M, Zhou J, Chen YJ, Bai LJ (2019) Voltammetric aptasensor for sulfadimethoxine using a nanohybrid composed of multifunctional fullerene, reduced graphene oxide and Pt@ Au nanoparticles, and based on direct electron transfer to the active site of glucose oxidase. Microchim Acta 186:1

9. Gooding JJ, Wibowo R, Liu JQ, Yang WR, Losic D, Orbons S, Mearns FJ, Shapter JG, Hibbert DB (2003) Protein electrochemistry using aligned carbon nanotube arrays. J Am Chem Soc 125: 9006–9007

10. Deng S, Jian G, Lei J, Hu Z, Ju H (2009) A glucose biosensor based on direct electrochemistry of glucose oxidase immobilized on nitrogen-doped carbon nanotubes. Biosens Bioelectron 25:373–377

11. Liu Y, Wang M, Zhao F, Xu Z, Dong S (2005) The direct electron transfer of glucose oxidase and glucose biosensor based on carbon nanotubes/chitosan matrix. Biosens Bioelectron 21:984–988

12. Liu S, Ju H (2003) Reagentless glucose biosensor based on direct electron transfer of glucose oxidase immobilized on colloidal gold modified carbon paste electrode. Biosens Bioelectron 19:177–183

13. Lim SH, Wei J, Lin J, Li Q, KuaYou J (2005) A glucose biosensor based on electrodeposition of palladium nanoparticles and glucose oxidase onto Nafion-solubilized carbon nanotube electrode. Biosens Bioelectron 20:2341–2346

14. Bao SJ, Li CM, Zang JF, Cui XQ, Qiao Y, Guo J (2008) New nanostructured TiO$_2$ for direct electrochemistry and glucose sensor applications. Adv Funct Mater 18:591–599

15. Yang Z, Ren Y, ZhangY LJ, Li H, Hu XH, Xu Q (2011) Nanoflake-like SnS$_2$ matrix for glucose biosensing based on direct electrochemistry of glucose oxidase. Biosens Bioelectron 26:4337–4341

16. BalasubramanianK BM (2006) Biosensors based on carbon nanotubes. Anal Bioanal Chem 385:452–468

17. Li ZJ, Sheng LY, Meng AL, Xie CC, Zhao K (2016) A glassy carbon electrode modified with a composite consisting of reduced graphene oxide, zinc oxide and silver nanoparticles in a chitosan matrix for studying the direct electron transfer of glucose oxidase and for enzymatic sensing of glucose. Microchim Acta 183:1625–1632

18. Jose MV, Marx S, Murata H, Koepsel RR, Russell AJ (2012) Direct electron transfer in a mediator-free glucose oxidase-based carbon nanotube-coated biosensor. Carbon 50:4010–4020

19. Guiseppi-Elie A, Lei C, Baughman RH (2002) Direct electron transfer of glucose oxidase on carbon nanotubes. Nanotechnology 13:559–564

20. Wang Y, Liu L, Li M, Xu S, Gao F (2011) Multifunctional carbon nanotubes for direct electrochemistry of glucose oxidase and glucose bioassay. Biosens Bioelectron 30:107–111

21. Luong JH, Glennon JD, Gedanken A, Vashist SK (2017) Achievement and assessment of direct electron transfer of glucose oxidase in electrochemical biosensing using carbon nanotubes,

graphene, and their nanocomposites. Microchim Acta 184:369–388

22. Chen RJ, Zhang Y, Wang D, Dai H (2001) Noncovalent sidewall functionalization of single-walled carbon nanotubes for protein immobilization. J Am Chem Soc 123:3838–3839

23. Sprafke JK, Stranks SD, Warner JH, Nicholas RJ, Anderson HL (2011) Noncovalent binding of carbon nanotubes by porphyrin oligomers. Angew Chem Int Ed 50:2313–2316

24. Bao SJ, Li CM, Guo CX, Qiao Y (2008) Biomolecule-assisted synthesis of cobalt sulfide nanowires for application in supercapacitors. J. Power Sources 180:676–681

25. Lin JY, Liao JH, Chou SW (2011) Cathodic electrodeposition of highly porous cobalt sulfide counter electrodes for dye-sensitized solar cells. Electrochim Acta 56:8818–8826

26. Chen CY, Shih ZY, Yang Z, Chang HT (2012) Carbon nanotubes/ cobalt sulfide composites as potential high-rate and high-efficiency supercapacitors. J. Power Sources 215:43–47

27. Willner B, Katz E, Willner I (2006) Electrical contacting of redox proteins by nanotechnological means. Curr Opin Biotechnol 17:589–596

28. Shan D, Zhang J, Xue HG, Ding SN, CosnierS (2010) Colloidal laponite nanoparticles: extended application in direct electrochemistry of glucose oxidase and reagentless glucose biosensing. Biosens Bioelectron 25:1427–1433

29. Wang L, Li J, Pan YF, Min LF, Zhang YC, Hu XY, Yang ZJ (2017) Platinum nanoparticle-assembled nanoflake-like tin disulfide for enzyme-based amperometric sensing of glucose, Microchim. Acta 184:2357–2363

30. Liu Q, Lu X, Li J, Yao X, Li J (2007) Direct electrochemistry of glucose oxidase and electrochemical biosensing of glucose on quantum dots/carbon nanotubes electrodes. Biosens Bioelectron 22:3203–3209

31. Liu Y, Wang MK, Zhao F, Hu ZA, Dong SJ (2005) The direct electron transfer of glucose oxidase and glucose biosensor based on carbon nanotubes/chitosan matrix. Biosens Bioelectron 21:984988

32. Wen ZH, Ci SQ, Li JH (2009) Pt nanoparticles inserting in carbon nanotube arrays: Nanocomposites for glucose biosensors. J Phys Chem C 113:13482–13487

33. Wang K, Liu Q, Guan QM, Wu J, Li HN, Yan JJ (2011) Enhanced direct electrochemistry of glucose oxidase and biosensing for glucose via synergy effect of graphene and CdS nanocrystals. Biosens Bioelectron 26:2252–2257

34. Shuai Y, Liu C, Wang J, Cui X, Nie L (2013) Pseudo-bi-enzyme glucose sensor: ZnS hollow spheres and glucose oxidase concerted catalysis glucose. Analyst 138:3259–3263

35. Li J, Lu MM, Xu YB, Zhang YC, Hu XY, Yang ZJ (2016) One-step solvothermal preparation of silver-ZnO hybrid nanorods for use in enzymatic and direct electron-transfer based biosensing of glucose. Microchim Acta 183:1705–1712